NANO LETTERS

pubs.acs.org/NanoLett

Letter

Building Reversible Nanoraspberries

E. Deniz Eren, Mohammad-Amin Moradi, Heiner Friedrich, and Gijsbertus de With*

Cite This: *Nano Lett.* 2021, 21, 2232−2239

Read Online

ACCESS | Metrics & More | Article Recommendations | Supporting Information

ABSTRACT: The adsorption mechanism of small positively charged silica nanoparticles (SiO_2 NPs) onto larger polystyrene latex nanoparticles (PSL NPs) forming hybrid particles was studied. CryoTEM showed the morphology of these supraparticles to be raspberry-like. After surface modification of the SiO_2 NPs, the optimum pH regime to initiate the formation of nanoraspberries was determined. Thereafter, their size evolution was evaluated by dynamic light scattering for different surface charge densities. Reversibility of nanoraspberry formation was shown by cycling the pH of the mixture to make interparticle forces either attractive or repulsive, while their stability was confirmed experimentally. The number of SiO_2 NPs on the PSL NPs as determined with cryoTEM matched the theoretically expected maximum number. Understanding and controlling the relevant parameters, such as size and charge of the individual particles and the Debye length, will pave the way to better control of the formation of nanoraspberries and higher-order assemblies thereof.

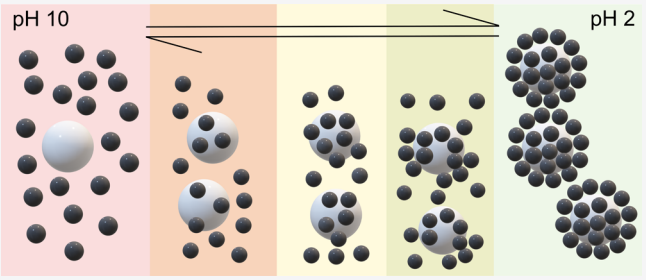

KEYWORDS: *Supraparticles, Raspberry Nanoparticles, Self-assembly, Silica Nanoparticles, CryoTEM*

INTRODUCTION

Small, simple building blocks can assemble into disordered or ordered complex structures in nature[1,2] or in a laboratory.[3,4] If these building blocks assemble into complex ordered structures without human intervention, it is called self-assembly.[5] Myriads of complex structures can be formed via self-assembly, such as colloidal crystals,[4] lipid bilayers,[6] cytoskeletons of cells,[7] and virus capsids.[8] Self-assembly can be induced in binary colloidal systems to form stable raspberry-like structures by finely balancing the attractive and repulsive forces between them. Although it sounds like a simple task, the formation of raspberry particles requires a good understanding and control of the critical forces responsible for tuning the kinetics of the assembly process.

In order to force small nanoparticles to attach onto the surface of a larger nanoparticle to create a raspberry nanoparticle, one needs to be aware of the importance of the key parameters governing the behavior of individual nanoparticles in the solution. The formation of raspberry nanoparticles can be induced if attractive interactions between the different nanoparticles overcome the repulsive interactions.[9] Various types of raspberry particles consisting of organic and inorganic nanoparticles have been created on varying length scales by tuning the process conditions, such as ionic strength, pH, type of solvent, and temperature.[10−15] Importantly, electrostatic interactions[16] between individual nanoparticles play a crucial role in their self-assembly. Electrostatic interactions between individual nanoparticles are highly susceptible to the ionic strength and pH of the solution, which opens new possibilities to control the self-assembly of individual nanoparticles, and thus control over the formation of raspberry nanoparticles.[10,17] Consequently, the key aspect of controlling the formation of nanoraspberries is to understand and manipulate the attractive and repulsive forces governing the behavior of different building blocks. To that end, understanding and controlling the stability of SiO_2 NPs, the PSL NPs, and the nanoraspberries, as well as the aggregation dynamics of the nanoraspberries as a function of pH and ionic strength of the solution, will be the focus of this paper.

In the past, adsorption phenomena of oppositely charged spherical colloidal particles[12−15,18,19] have been studied intensively. Vincent et al.[13] studied the deposition of positively charged polystyrene latex microspheres onto negatively charged polystyrene latex particles and examined the effect of poly(vinyl alcohol) and ionic strength on the deposition kinetics of small particles. Similarly, Harley et al.[14] showed the adsorption of small, negatively charged latex nanoparticles onto larger, positively charged latex particles by employing a new thin-film, freeze-drying/scanning electron microscopy technique. More recently it has been shown that deposition of different organic and inorganic nanoparticles onto larger latex particles can be achieved.[20−23] Sadowska et al. showed that deposition of positively charged 100 nm polystyrene latex

Received: December 23, 2020
Revised: February 16, 2021
Published: February 18, 2021

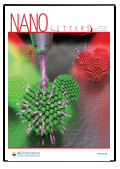

https://dx.doi.org/10.1021/acs.nanolett.0c05059
Nano Lett. 2021, 21, 2232−2239

nanoparticles onto negatively charged 820 nm polystyrene latex particles can be initiated by adjusting the ionic strength of the solution.[21] In another study by Sadowska et al., it was demonstrated that the coverage of larger polystyrene latex particles by smaller silver nanoparticles[22] can be controlled to a certain degree by controlling the ionic strength of the solution. In still other studies, in line with the above-mentioned works, the coverage of polystyrene microspheres by different inorganic nanoparticles has been demonstrated.[20,24] Using a different strategy, Lan et al.[25] showed a method where they synthesized raspberry colloids by injecting at 70 °C a mixture of acrylate monomers, styrene, and the cross-linker divinylbenzene into a water−ethanol solution (80/20 v/v) containing the initiator 2,2′-azobis(2-methylpropionamide) dihydrochloride. Due to the solubility differences of styrene and acrylate monomers in the water−ethanol mixture, dispersion polymerization of the acrylate monomers and surfactant-free emulsion polymerization of styrene-rich emulsion droplets occurred simultaneously, which resulted in the formation of ∼45 nm polyacrylate and ∼200 nm polystyrene particles. Thereafter, these nanoparticles fused, thereby creating raspberry colloids in the presence of the cross-linker. They found that the solvent conditions and the concentration of cross-linker were crucial in the formation process of the raspberry particles. Recently, we showed that the enthalpy-driven self-assembly of particles at low concentration and the entropy-driven packing of particles at high concentration can be combined into a single strategy to achieve three-dimensional structured multicomponent materials.[26] Last but not least, raspberry-like particles consisting of an organic and an inorganic component can play a crucial role in the rational design of the hybrid materials, possibly to be used in applications such as catalysts,[27] plasmonics,[28] and biodevices.[29]

The main goal of this paper is to monitor the aggregation dynamics and elucidate the driving forces of adsorption of silica nanoparticles (SiO_2 NPs) on polystyrene latex nanoparticles (PSL NPs). The covering process by the SiO_2 NPs is determined under *in situ* conditions via time-resolved cryoTEM and dynamic light scattering experiments. By cycling the pH of the mixture to make interparticle forces either attractive or repulsive, we show the reversibility of nanoraspberry formation.

EXPERIMENTAL SECTION

Aqueous suspensions of negatively charged PSL spheres were obtained from either Sigma-Aldrich (LB1) or Fisher Scientific (Distrilab) and were used as received. Ultrapure water (with a resistivity of 18 MΩ cm obtained using a Milli-Q water purifier) was used in all experiments. A stock dispersion was prepared by diluting the PSL NPs dispersion 1:10 with ultrapure water. SiO_2 NPs were synthesized according to previously described methods[30,31] (see the Supporting Information, Materials and Methods). Size and surface charge characterizations of the as-synthesized SiO_2 NPs were conducted using dynamic light scattering (Zeta-sizer, Malvern). As-synthesized silica nanoparticles are negatively charged over a broad range of solution conditions. In order to facilitate charge reversal by changing the pH, a previously published surface functionalization method was employed[32] (see Supporting Information, Materials and Methods). In order to perform the reversibility experiments, the amount of buffer necessary was calculated based on the desired ionic strength for the specific sample volume (Table S1).

Cryogenic transmission electron microscopy (cryoTEM) and dynamic light scattering (DLS) were employed to measure the size distribution of silica nanoparticles and to monitor the evolution of the hydrodynamic diameter of the aggregates as a function of surface charge density as determined by zeta potential measurements. CryoTEM samples were prepared by depositing 3 μL samples on a 200 mesh Cu grid with Quantifoil R2/2 holey carbon film (Quantifoil Micro Tools GmbH) or Lacey/Carbon 200 mesh (Electron Microscopy Sciences). All TEM grids were surface plasma treated for 40 s using a Cressington 208 carbon coater prior to use. An automated vitrification robot (Fisher Scientific Vitrobot Mark IV) was used for plunge vitrification in liquid ethane. CryoTEM studies were performed on a TU/e cryoTITAN instrument (Thermo Fisher Scientific) operated at 300 kV, equipped with a field emission gun (FEG), a post-column Gatan Energy Filter (GIF), and a post-GIF 2k × 2k Gatan CCD camera. The size and SiO_2 NP coverage of the supraparticles which have the raspberry-like morphology were measured from the cryoTEM images by typically using 250 particles.

DLS was used to determine the number weighted size distribution, electrophoretic mobility, and zeta potential of the silica nanoparticles, as well as the polystyrene latex nanoparticles, employing the Debye approximation. Size evolution and corresponding zeta potential values of the nanoraspberries for a given surface charge density were also monitored in time and with varying pH. The sizes of the PSL NPs, SiO_2 NPs, and nanoraspberries are reported as the mean ± the standard deviation of the mean.

The zeta potential, electrophoretic mobility, and size distribution of the SiO_2 NPs and PSL NPs were determined to better understand the behavior of the individual nanoparticle systems. The conversion from electrophoretic mobility to zeta potential was done by employing the Henry equation using the Smoluchowski approximation as appropriate for aqueous dispersions.[33] The size of the SiO_2 NPs determined from cryoTEM was 28.8 ± 0.4 nm (Figures SI1a, SI1b, and SI1c) and 30.2 ± 0.8 nm according to DLS (Figure SI1d). At this point, it is important to note that the size of the silica nanoparticles as measured by cryoTEM is often smaller than the size measured by DLS. Although frequently the size measured by DLS shows a somewhat larger value than that measured by microscopy,[34] this is not always the case.[35] Generally, a comparison of the results of these methods is not straightforward at all.[36−38] DLS was employed to analyze the PSL NPs which showed a hydrodynamic diameter of 100 ± 9 nm (Figure SI2).

RESULTS AND DISCUSSION

Zeta potential measurements (Figure 1a) were conducted to determine the surface charges of the individual nanoparticle samples and to prove that the surface modification process resulted in SiO_2 NPs with reversible charge. Before surface modification, the SiO_2 NPs were only negatively charged over the pH range of 3−9, while after surface modification the surface of the SiO_2 NPs became positively charged below a pH of approximately 5.5. The same technique was employed to determine the surface charge of the PSL NPs and for the whole pH range considering that the PSL NPs respond to pH changes but remain in a range approximately between −40 and −60 mV (Figure 1a).

https://dx.doi.org/10.1021/acs.nanolett.0c05059
Nano Lett. 2021, 21, 2232−2239

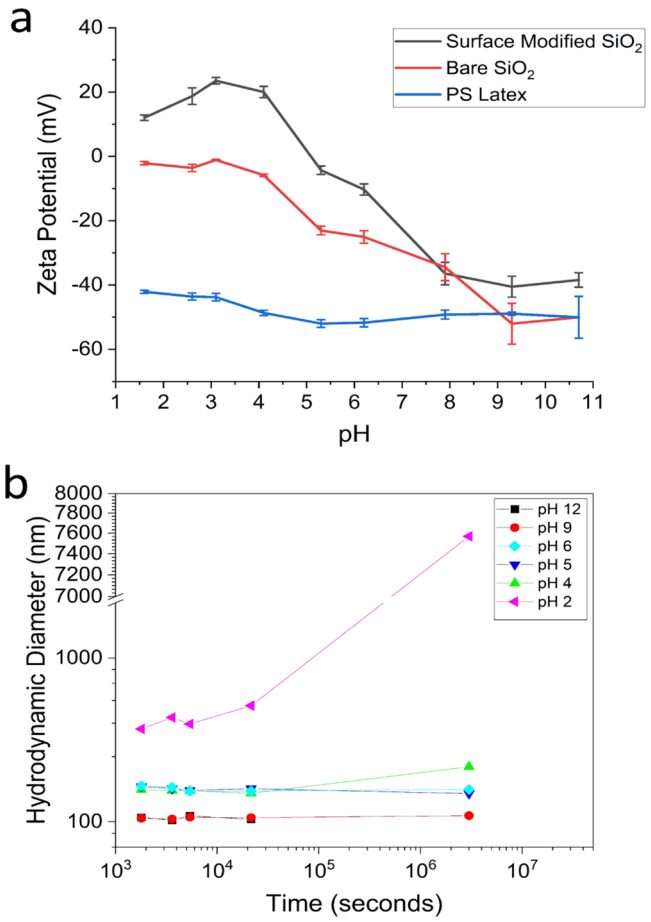

Figure 1. (a) Zeta potential measurements of PSL NPs, bare SiO_2 NPs, and surface-modified SiO_2 NPs. (b) Evolution of the hydrodynamic diameter of aggregates in a mixture of 30 nm surface-modified SiO_2 NPs and 100 nm PSL NPs at different pH values over time. Results for pH 9 and pH 12 overlap for the whole range as they do for pH 5 and 6. The lines drawn are a guide to the eye.

In order to determine the most efficient pH range to initiate self-assembly between the PSL NPs and SiO_2 NPs, time-resolved DLS experiments were conducted to monitor the formation of aggregates as a function of time at pH values ranging from 2 to 12 (Figures 1b, Figures SI3 and SI4). The DLS results show that at pH 12 and pH 9, the hydrodynamic diameter of the hybrid particles does not change and is constant over time at 105 ± 4 nm (for details, see Figures SI3 and SI4). This constant value of the hydrodynamic diameter at pH 12 and pH 9 over 10^6 s (or about 1 month) clearly suggests that the PSL NPs and SiO_2 NPs do not attach to each other owing to repulsive Coulomb interactions at this specific pH range. At pH 6 and pH 5 the hydrodynamic diameter for the mixture of SiO_2 NPs and PSL NPs also shows a constant hydrodynamic diameter over a period of 1 month, but now at a value of 158 ± 5 nm, which is thus significantly larger than that of the bare PSL. At pH 4 the measured hydrodynamic diameter is 152 ± 3 nm; it does not change initially after mixing but increases to 216 ± 4 nm after 1 month. This can be explained by the low zeta potential value for the hybrid particles at pH 4 which was measured to be +6 ± 0.3 mV. The fact that these hybrid particles are positively charged indicates that positively charged SiO_2 NPs are partly covering the negatively charged surfaces of PSL NPs. Finally, the hydrodynamic diameter results obtained from a mixture at pH 2 indicates that the PSL NPs and SiO_2 NPs are highly attractive at this pH. They form hybrid particles already 2 min after mixing for which the hydrodynamic diameter was measured to be 257 nm and increasing to many micrometers after one month (Figure 1b, pink triangles). Although a precise interpretation of DLS and zeta potential data cannot be expected as their prerequisites are not completely fulfilled, they nevertheless offer sufficient guidance to explain the mechanism.

In summary, three different regimes can be observed from the DLS results: (1) a regime where the particle diameter stays constant at the size of the PSL NPs, suggesting that individual nanoparticles do not interact with each other (Figure 1b; black squares and red circles); (2) a regime where the particle diameter increased in size relative to the PSL NPs, suggesting that individual nanoparticles form hybrid particles due to the attractive Coulomb forces (Figure 1b; green, blue, and turquoise triangles); and (3) a regime in which the particle diameter increases far beyond the PSL NP size, indicating that large aggregates are formed in time (Figure 1b; pink triangle). This has been confirmed with cryoTEM, which also shows their raspberry-like morphology for pH 4 (Figure 2a, 2b) and pH 2 after 2 min of mixing the PSL NPs and SiO_2 NPs (Figure 2c–h), with PSL NPs partly covered with SiO_2 NPs (Figure 2c, 2d, 2e) as well as with PSL NPs fully covered with SiO_2 NPs (Figure 2f, 2g, 2h).

CryoTEM results also show that 1 week after mixing at pH 2 the PSL NPs and SiO_2 NPs form networks of well-defined nanoraspberries with the PSL NPs fully covered with SiO_2 NPs (Figure 2i, 2j). Moreover, DLS results at pH 2 clearly show a gradual increase of the hydrodynamic diameter over time. After 6 h, the hydrodynamic diameter was measured as 511 nm, indicating that several nanoraspberries were attached to each other. Finally, the DLS results after 1 month show that the hydrodynamic diameter at pH 2 increased to 7600 nm, indicating that the nanoraspberries are forming agglomerates, as proved via cryoTEM (Figure 2k, 2l, and enveloped with yellow borders in Figure 2m).

To compare the experimental results for the number of SiO_2 NPs on the surface of PSL NPs, we used a theoretical estimate as given by Mansfield et al.[39] They studied how many "probe" (small) spheres on average can be attached to a "target" (large) sphere by a random attachment process until all available sites on the surface of the target sphere are exhausted. In this calculation the authors either allowed mobility of the small spheres attached to the large sphere or not, ultimately resulting in small differences, and we assume here immobile small spheres. The mean number of the small spheres M that can be attached is given by

$$M = K\left(\frac{r_1}{r_2} + 1\right)^2$$

with the constant $K = 2.187 \pm 0.004$.[39] By using this model, we calculated M and compared these results with the experimental results obtained from cryoET (Movie S1). It appears that the number of SiO_2 NPs attached to the surface of PSL NPs can be predicted quite accurately. For example, in the case of the single nanoraspberry shown in Figure 3, the theoretical prediction shows that the number of small particles attached to the surface of the large particle should be $M^{theor} = 55.5$, while cryoET results demonstrate that $M^{exp} = 54$. The excellent

https://dx.doi.org/10.1021/acs.nanolett.0c05059
Nano Lett. 2021, 21, 2232−2239

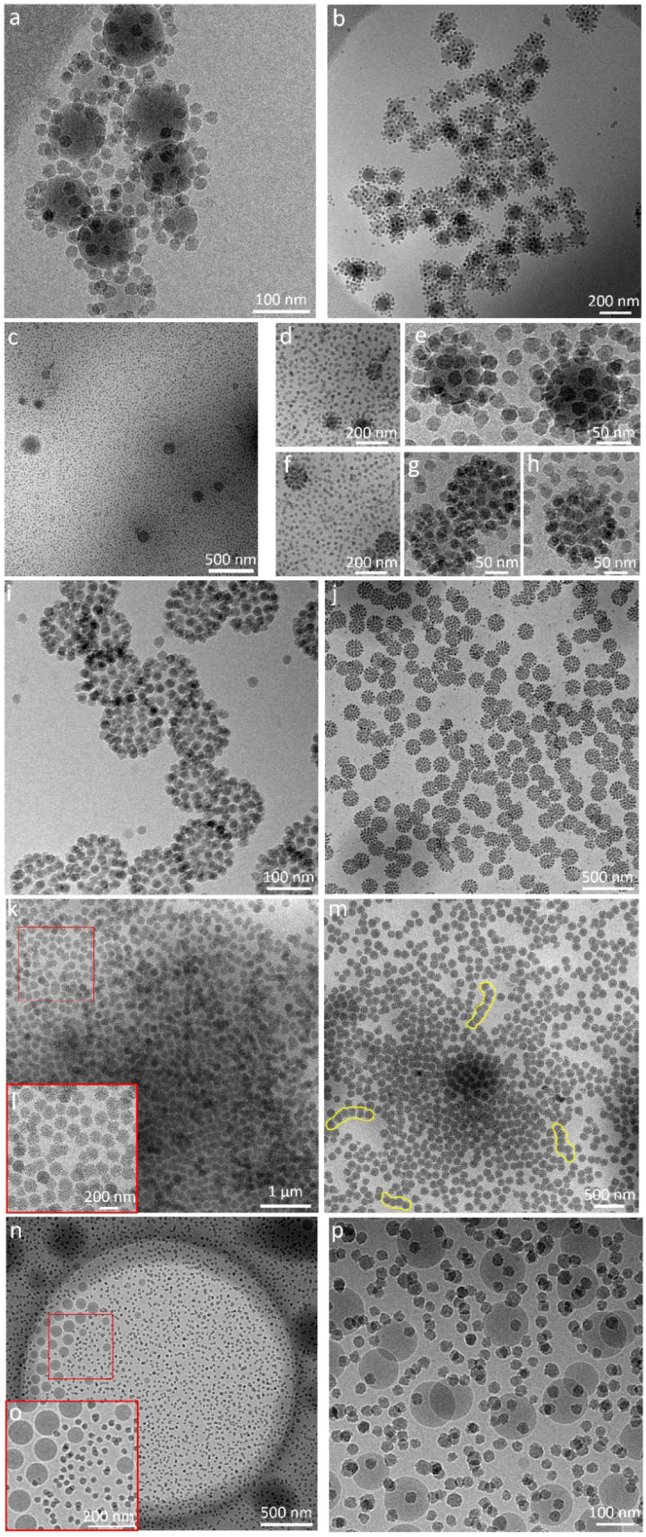

Figure 2. CryoTEM images of the mixture of PSL NPs and SiO_2 NPs (a, b) at pH 4 taken 1 month after mixing and (c–h) at pH 2 taken 2 min after mixing. In this case, several images are shown to demonstrate clearly in detail that the PSL NPs are not fully covered with SiO_2 NPs yet (i, j) at pH 2 taken 1 week after mixing, (k–m) at pH 2 taken 1 month after mixing, and (n–p) at pH 12 taken 1 month after mixing.

agreement between the experimental and theoretical *M* values is also a good indicator that equilibrium was reached.

At this point, one needs to consider that the stability of colloidal particles in a solution depends on the balance between attractive van der Waals and repulsive double-layer forces. It is also important to note that at higher salt concentrations bridging of nanoraspberries by SiO_2 NPs could occur. Consequently, insufficient repulsive forces will eventually result in an unstable colloidal suspension where nanoparticles stick to each other due to van der Waals forces.[16] The zeta potential boundary between stable and nonstable colloids is considered to be ±25 or ±30 mV.[40] Hence, in order to determine the stability and cyclability of the nanoraspberry assembly, electrophoretic mobility and zeta potential measurements were conducted (Figure SI5).

The zeta potential can be linked to the surface charge and can change due to changes in pH or due to the salt content of the medium. Results obtained from the mixture at pH 2 demonstrate that the zeta potential of the solution is +21 mV (Figure SI5a). Because the SiO_2 NPs were surface modified by APTES molecules, the amine moieties on the surface of the SiO_2 NPs are protonated at pH 2. Therefore, we can conclude that the surface of PSL NPs was fully covered by SiO_2 NPs. The behavior of individual PSL NPs and SiO_2 NPs is quite different at pH 4, pH 5, and pH 6 as compared to that at pH 2. The zeta potentials of mixtures measured after 1 week at pH 4, pH 5, and pH 6 were +6 ± 0.3 mV, −5 ± 0.7 mV, and −4 ± 0.3 mV, respectively (Figure SI5a).

These results indicate that PSL NPs and SiO_2 NPs have limited interaction with each other, as corroborated by the hydrodynamic diameter measurements. Zeta potential measurements at pH 9 and pH 12 for the mixtures show highly negatively charged particles, which is in line with the zeta potential measurements of the individual PSL NPs and SiO_2 NPs. Individual nanoparticle systems also have a negatively charged surface at higher pHs, making it impossible for them to form nanoraspberries upon mixing (Figure 2n–p).

Furthermore, the reversible and dynamic nature of the nanoraspberries was evaluated via cryoTEM and DLS by adjusting the pH of the mixture (Figure 4). First, PSL NPs and SiO_2 NPs were mixed at neutral pH which was thereafter dropped to pH 2 by adding a mixture of 0.1 M KCl (50 mL) and 0.1 M HCl (13 mL)[41,42] in order to initiate the formation of nanoraspberries (Figure 4a). CryoTEM results indicate that the formation of nanoraspberries was successful and that they were efficiently separated from each other. Subsequently, the pH was increased to 10 by adding a mixture of 0.2 M KCl (50 mL) and 0.2 M NaOH (12 mL) in order to investigate whether the nanoraspberries would stay intact or individual, separated PSL NPs and SiO_2 NPs would be observed. CryoTEM results obtained at pH 10 demonstrate that separated PSL NPs and SiO_2 NPs are observed, indicating that the nanoraspberries fully dissociated and that the PSL NPs and SiO_2 NPs repel each other (Figure 4b); however, some small clusters of silica NPs can be observed. In order to fully understand the presence of small clusters of silica NPs, we conducted a series of zeta potential experiments to evaluate the behavior of the mixture upon altering the pH. The most striking result found was the gradual decrease of the zeta potential of the solution upon increasing the pH from 2 to 10 during the first cycle (Figure 4e, the transition from a to b). This is important because the second increase of the pH from 2 to 10 occurred very steeply (Figure 4e, the transition from c to d), resulting in an immediate negatively charged mixture. This might explain why we observed some clusters of SiO_2

https://dx.doi.org/10.1021/acs.nanolett.0c05059
Nano Lett. 2021, 21, 2232–2239

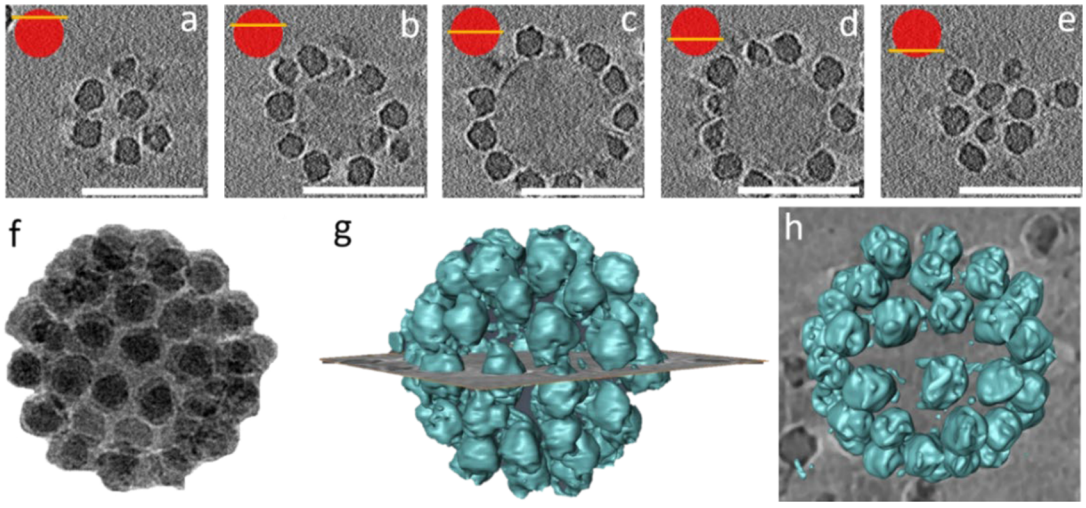

Figure 3. Cross sections at different heights in a nanoraspberry as obtained from cryoET reconstructions (a–e) show that the PSL nanoparticle is fully covered with SiO_2 NPs. Scale bars = 100 nm. Further, (f) shows the cryoTEM image of a single nanoraspberry, and (g) and (h) show the side and top view of the 3D reconstruction of the same nanoraspberry, respectively.

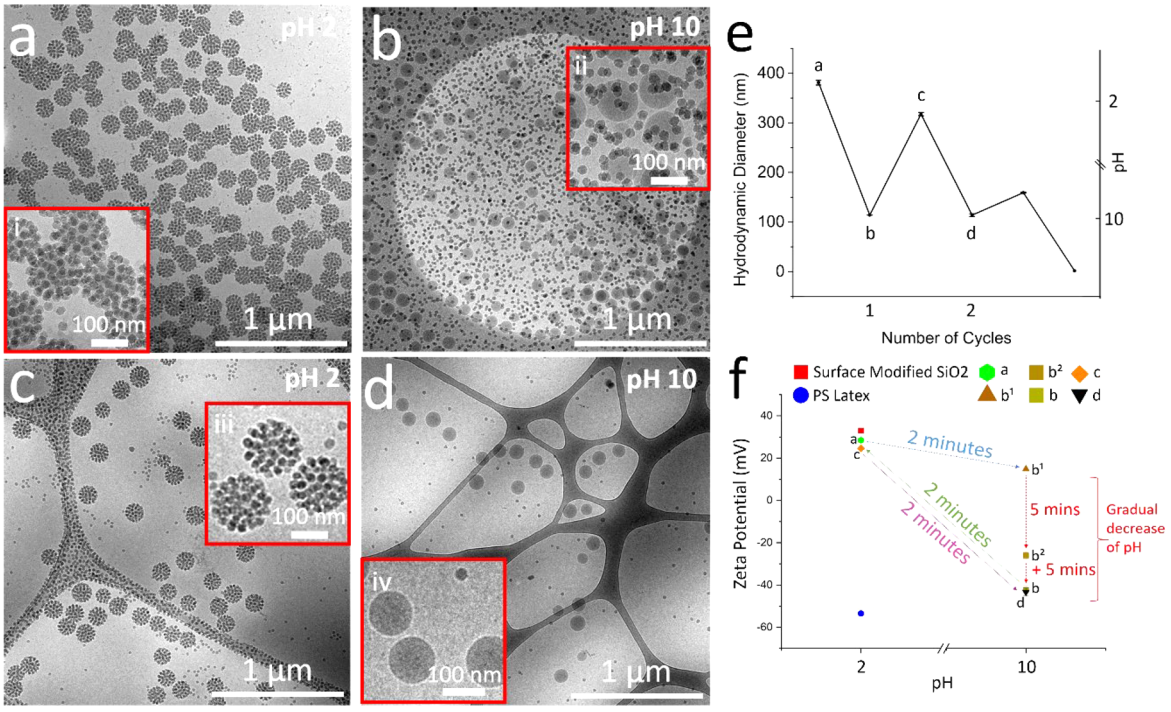

Figure 4. Dynamic and reversible nature of nanoraspberries as evaluated by cryoTEM characterization made by surface-modified SiO_2 NPs mixed with PSL NPs. (a) Mixture at pH 2. (b) The mixture as shown in (a) brought at pH 10. (c) The mixture shown in (b) brought at pH 2 again. (d) The mixture shown in (c) brought back to pH 10 again. (e) DLS results at various pH corresponding to the cryoTEM images (a) to (d) (see also Figure SI6b). The error bars indicate the standard deviation in the mean, which is typically 10 nm. (f) Zeta potential measurements for PSL NPs, SiO_2 NPs, and mixtures used in the reversibility experiments as a function of pH.

NPs still sticking to each other to create chain-like structures (Figure 4b). Although we were always very meticulous while conducting the experiments, waiting until solutions reached equilibrium before conducting the imaging experiments, one can infer from Figure 4f that due to the gradual decrease of zeta potential during the transition from pH 2 to 10 (the transition from a to b), the mixture may not have reached equilibrium yet and that some of the SiO_2 NPs are still in contact with each other.

Thereafter, for the same solution, the pH was adjusted from 10 to 2 (the transition from b to c), for which cryoTEM results confirmed the reformation of nanoraspberries (Figure 4c). Finally, the pH was increased to 10 (the transition from c to d) again in order to observe whether they disassociate again. CryoTEM imaging demonstrated that the nanoraspberries indeed dissociate again, indicating that the individual particles are repelling each other (Figure 4d) and supporting the results obtained from DLS (Figure 4f). Taking everything into consideration, this demonstrates the reversible nature of this particle system.

The pH was dropped once more to 2 to monitor the possible structural alteration of the mixture. Consistent with

https://dx.doi.org/10.1021/acs.nanolett.0c05059
Nano Lett. 2021, 21, 2232–2239

the hydrodynamic radius for further cyclability experiments (Figure SI6), the structure was much less well defined. Hence, although the behavior of the nanoraspberries was designated as reversible above, after all, it may be better to label it as pseudoreversible. As upon repeating the pH cycle, the ionic strength inevitably increases, and at some point the reversibility is terminated. An important parameter to consider in this respect is the Debye length κ^{-1}, which is a measure of the range of electrostatic effects in a solution for a given charged particle (eq 1) given by

$$\kappa^2 = 2e^2 I/\varepsilon_r \varepsilon_0 kT \quad (1)$$

with e (C) being the elementary charge, ε_0 (F m^{-1}) the vacuum permittivity, ε_r (−) the relative permittivity (dielectric constant) of the medium, k (J K^{-1}) the Boltzmann constant, and T (K) the temperature. Further, the ionic strength I is given by

$$I = \frac{1}{2}\sum_{j=1}^{n} c_j z_j^2 \quad (2)$$

Here, c_j (M, mol L^{-1}) is the molar concentration of ion j, and z_j is the charge number of that ion. The number $\frac{1}{2}$ accounts for the fact that both cations and anions are included. Thus, for a given aqueous solution containing charged PSL NPs and SiO_2 NPs at room temperature, the Debye length is only dependent on the ionic strength, meaning that by adjusting cyclically the pH, the double layer of the individual particles is continuously compressed up to a certain point, after which they are more or less fully screened (Figure 5).

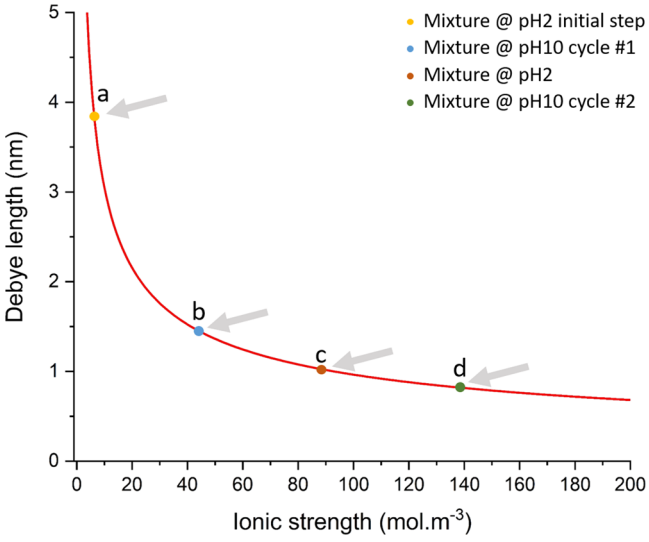

Figure 5. Influence of changing ionic strength I on the Debye length κ^{-1} in water at a 25 °C. Ionic strength values corresponding to cycling steps in Figure 4 shown as a, b, c, and d.

CONCLUSIONS

In summary, it was demonstrated that the preparation of nanoraspberries, with PSL NPs of about 100 nm acting as the core and SiO_2 NPs of about 30 nm providing the shell, was achieved. The key is that the formation of nanoraspberries is highly dependent on the interaction strength between individual nanoparticles in the solution, and therefore, one can control the formation of supraparticles by simply tuning the ionic strength of the solution. Moreover, our results show that the distribution of SiO_2 NPs over the PSL NPs can be controlled by adjusting the pH of the medium. It was demonstrated via cryoTEM that the electrostatic interaction between the supraparticles is not strong enough to prevent them to be separated over one month, even if the required pH is maintained. Furthermore, the (pseudo)reversible nature of these nanoraspberries was shown by cycling the pH between 2 and 10. Cycling obviously increases the ionic strength, and above a critical ionic strength of the solution (approximately 140 mol m^{-3}), nanoraspberries cannot reassemble anymore, as a high salt concentration implies a small Debye screening length and therefore short-ranged interaction forces. Finally, from the experimental data the number of small SiO_2 NPs on the surface of a large PSL NP was determined, showing a good agreement with the theoretical calculations.

ASSOCIATED CONTENT

Supporting Information

The Supporting Information is available free of charge at https://pubs.acs.org/doi/10.1021/acs.nanolett.0c05059.

Additional experimental details, synthesis and surface modification of silica nanoparticles, size measurements of silica and polystyrene latex nanoparticles, pseudoreversibility of nanoraspberries, and theoretical considerations (PDF)

Movie S1 (AVI)

AUTHOR INFORMATION

Corresponding Author

Gijsbertus de With − *Laboratory of Physical Chemistry, Department of Chemical Engineering and Chemistry, Eindhoven University of Technology, 5600MB Eindhoven, The Netherlands;* orcid.org/0000-0002-7163-8429; Email: G.deWith@tue.nl

Authors

E. Deniz Eren − *Laboratory of Physical Chemistry, Department of Chemical Engineering and Chemistry, Eindhoven University of Technology, 5600MB Eindhoven, The Netherlands*

Mohammad-Amin Moradi − *Laboratory of Physical Chemistry, Department of Chemical Engineering and Chemistry, Eindhoven University of Technology, 5600MB Eindhoven, The Netherlands;* orcid.org/0000-0003-3754-9200

Heiner Friedrich − *Laboratory of Physical Chemistry, Department of Chemical Engineering and Chemistry, Eindhoven University of Technology, 5600MB Eindhoven, The Netherlands; Institute for Complex Molecular Systems, Eindhoven University of Technology, 5600MB Eindhoven, The Netherlands;* orcid.org/0000-0003-4582-0064

Complete contact information is available at: https://pubs.acs.org/10.1021/acs.nanolett.0c05059

Author Contributions

E.D.E. and M-A.M. designed and carried out all the experiments. G.d.W. and H.F. supervised the data analysis; E.D.E. and M-A.M. carried out the data analysis. G.d.W. supervised the project, and E.D.E. and G.d.W. wrote the

https://dx.doi.org/10.1021/acs.nanolett.0c05059
Nano Lett. 2021, 21, 2232−2239

manuscript with contributions from all authors. All authors discussed the results and commented on the manuscript.

Notes

The authors declare no competing financial interest.

■ ACKNOWLEDGMENTS

E.D.E. was supported by the EU H2020 Marie Sklodowska-Curie Action project MULTIMAT. M-A.M. was supported by the 4TU High-Tech Materials research program New Horizons in Designer Materials.

■ REFERENCES

(1) Wegst, U. G. K.; Bai, H.; Saiz, E.; Tomsia, A. P.; Ritchie, R. O. Bioinspired structural materials. *Nat. Mater.* **2015**, *14*, 23−36.
(2) Grzybowski, B. A.; Wilmer, C. E.; Kim, J.; Browne, K. P.; Bishop, K. J. M. Self-assembly: From crystals to cells. *Soft Matter* **2009**, *5*, 1110−1128.
(3) Bollhorst, T.; Rezwan, K.; Maas, M. Colloidal capsules: Nano- and microcapsules with colloidal particle shells. *Chem. Soc. Rev.* **2017**, *46*, 2091−2126.
(4) Boles, M. A.; Engel, M.; Talapin, D. V. Self-assembly of colloidal nanocrystals: From intricate structures to functional materials. *Chem. Rev.* **2016**, *116*, 11220−11289.
(5) Whitesides, G. M.; Grzybowski, B. Self-assembly at all scales. *Science (Washington, DC, U. S.)* **2002**, *295*, 2418−2421.
(6) Mueller, P.; Rudin, D. O.; Ti Tien, H.; Wescott, W. C. Reconstitution of cell membrane structure in vitro and its transformation into an excitable system. *Nature* **1962**, *194*, 979−980.
(7) Fletcher, D. a.; Mullins, R. D. Cell mechanisms and cytoskeleton. *Nature* **2010**, *463*, 485−492.
(8) Perlmutter, J. D.; Hagan, M. F. Mechanisms of Virus Assembly. *Annu. Rev. Phys. Chem.* **2015**, *66*, 217−239.
(9) Manoharan, V. N. Colloidal matter: Packing, geometry, and entropy. *Science* **2015**, *349*, 1253751.
(10) Luo, D.; Yan, C.; Wang, T. Interparticle Forces Underlying Nanoparticle Self-Assemblies. *Small* **2015**, *11* (45), 5984−6008.
(11) Carcouët, C. C. M. C.; Esteves, A. C. C.; Hendrix, M. M. R. M.; van Benthem, R. A. T. M.; de With, G. Fine-Tuning of Superhydrophobicity Based on Monolayers of Well-defined Raspberry Nanoparticles with Variable Dual-roughness Size and Ratio. *Adv. Funct. Mater.* **2014**, *24*, 5745−5752.
(12) Vincent, B.; Jafelicci, M.; Luckham, P. F.; Tadros, T. F. Adsorption of Small, Positive Particles onto Large, Negative Particles in the Presence of Polymer. *J. Chem. Soc., Faraday Trans. 1* **1980**, *76*, 674−682.
(13) Vincent, B.; Young, C. A.; Tadros, T. F. Equilibrium Aspects of Heteroflocculation in Mixed Sterically-stabilised Dispersions. *Faraday Discuss. Chem. Soc.* **1978**, *65*, 296−305.
(14) Harley, S.; Thompson, D. W.; Vincent, B. The adsorption of small particles onto larger particles of opposite charge Direct electron microscope studies. *Colloids Surf.* **1992**, *62*, 163−176.
(15) Ming, W.; Wu, D.; van Benthem, R.; de With, G. Superhydrophobic films from raspberry-like particles. *Nano Lett.* **2005**, *5*, 2298−2301.
(16) Hueckel, T.; Hocky, G. M.; Palacci, J.; Sacanna, S. Ionic solids from common colloids. *Nature* **2020**, *580*, 487−490.
(17) Demirörs, A. F.; et al. Long-ranged oppositely charged interactions for designing new types of colloidal clusters. *Phys. Rev. X* **2015**, *5*, 1−12.
(18) Adamczyk, Z.; Warszyński, P. Role of electrostatic interactions in particle adsorption. *Adv. Colloid Interface Sci.* **1996**, *63*, 41−149.
(19) Caruso, F.; Lichtenfeld, H.; Giersig, M.; Mohwald, H. Electrostatic self-assembly of silica nanoparticle-polyelectrolyte multilayers on polystyrene latex particles [4]. *J. Am. Chem. Soc.* **1998**, *120*, 8523−8524.
(20) Oćwieja, M.; Lupa, D.; Adamczyk, Z. Gold Nanoparticle Layers on Polystyrene Microspheres of Controlled Structure and Electrokinetic Properties. *Langmuir* **2018**, *34*, 8489−8498.
(21) Sadowska, M.; Adamczyk, Z.; Nattich-Rak, M. Mechanism of nanoparticle deposition on polystyrene latex particles. *Langmuir* **2014**, *30*, 692−699.
(22) Sadowska, M.; Adamczyk, Z.; Oćwieja, M.; Nattich-Rak, M. Monolayers of silver nanoparticles on positively charged polymer microspheres. *Colloids Surf., A* **2016**, *499*, 1−9.
(23) North, S. M.; et al. Adsorption of Small Cationic Nanoparticles onto Large Anionic Particles from Aqueous Solution: A Model System for Understanding Pigment Dispersion and the Problem of Effective Particle Density. *Langmuir* **2017**, *33*, 1275−1284.
(24) Wagner, C. S.; Shehata, S.; Henzler, K.; Yuan, J.; Wittemann, A. Towards nanoscale composite particles of dual complexity. *J. Colloid Interface Sci.* **2011**, *355*, 115−123.
(25) Lan, Y.; Caciagli, A.; Guidetti, G.; Yu, Z. Y.; Liu, J.; Johansen, V. E.; Kamp, M.; Abell, C.; Vignolini, S.; Scherman, O. A.; Eiser, E. Unexpected stability of aqueous dispersions of raspberry-like colloids. *Nat. Commun.* **2018**, *9*, 3614.
(26) Moradi, M. A.; Eren, E. D.; Chiappini, M.; Rzadkiewicz, S.; Goudzwaard, M.; van Rijt, M. M. J.; Keizer, A. D. A.; Routh, A. F.; Dijkstra, M.; de With, G.; Sommerdijk, N. A. J. M.; Friedrich, H.; Patterson, J. P. Spontaneous organization of supracolloids into three-dimensional structured materials. *Nat. Mater.* **2021**, *1*−*7*, 1.
(27) Shirman, E.; et al. Modular Design of Advanced Catalytic Materials Using Hybrid Organic−Inorganic Raspberry Particles. *Adv. Funct. Mater.* **2018**, *28*, 1704559.
(28) Gandra, N.; Abbas, A.; Tian, L.; Singamaneni, S. Plasmonic planet-satellite analogues: Hierarchical self-assembly of gold nanostructures. *Nano Lett.* **2012**, *12*, 2645−2651.
(29) Chatterjee, K.; Sarkar, S.; Jagajjanani Rao, K.; Paria, S. Core/shell nanoparticles in biomedical applications. *Adv. Colloid Interface Sci.* **2014**, *209*, 8−39.
(30) Carcouët, C. C. M. C.; van de Put, M. W. P.; Mezari, B.; Magusin, P. C. M. M.; Laven, J.; Bomans, P. H. H.; Friedrich, H.; Esteves, A. C. C.; Sommerdijk, N. A. J. M.; van Benthem, R. A. T. M.; de With, G. Nucleation and Growth of Monodisperse Silica Nanoparticles. *Nano Lett.* **2014**, *14*, 1433−1438.
(31) Yokoi, T.; et al. Periodic arrangement of silica nanospheres assisted by amino acids. *J. Am. Chem. Soc.* **2006**, *128*, 13664−13665.
(32) Pham, K. N.; Fullston, D.; Sagoe-Crentsil, K. Surface charge modification of nano-sized silica colloid. *Aust. J. Chem.* **2007**, *60*, 662−666.
(33) Lowry, G. V.; et al. Guidance to improve the scientific value of zeta-potential measurements in nanoEHS. *Environ. Sci.: Nano* **2016**, *3*, 953−965.
(34) Souza, T. G. F.; Ciminelli, V. S. T.; Mohallem, N. D. S. A comparison of TEM and DLS methods to characterize size distribution of ceramic nanoparticles. *J. Phys.: Conf. Ser.* **2016**, *733*, 012039.
(35) Tuoriniemi, J.; et al. Intermethod comparison of the particle size distributions of colloidal silica nanoparticles. *Sci. Technol. Adv. Mater.* **2014**, *15*, 035009.
(36) Eaton, P.; et al. A direct comparison of experimental methods to measure dimensions of synthetic nanoparticles. *Ultramicroscopy* **2017**, *182*, 179−190.
(37) Amini, R.; Brar, S. K.; Cledon, M.; Surampalli, R. Y. Intertechnique Comparisons for Nanoparticle Size Measurements and Shape Distribution. *J. Hazard., Toxic Radioact. Waste* **2016**, *20*, 1−8.
(38) Bootz, A.; Vogel, V.; Schubert, D.; Kreuter, J. Comparison of scanning electron microscopy, dynamic light scattering and analytical ultracentrifugation for the sizing of poly(butyl cyanoacrylate) nanoparticles. *Eur. J. Pharm. Biopharm.* **2004**, *57*, 369−375.
(39) Mansfield, M. L.; Rakesh, L.; Tomalia, D. A. The random parking of spheres on spheres. *J. Chem. Phys.* **1996**, *105*, 3245−3249.

https://dx.doi.org/10.1021/acs.nanolett.0c05059
Nano Lett. 2021, 21, 2232−2239

(40) Greenwood, R. Review of the measurement of zeta potentials in concentrated aqueous suspensions using electroacoustics. *Adv. Colloid Interface Sci.* **2003**, *106*, 55−81.
(41) Maurer, G. Electrolyte solutions. *Fluid Phase Equilib.* **1983**, *13*, 269−296.
(42) Bower, V. E.; Bates, R. G. pH values of the Clark and Lubs buffer solutions at 25 C. *J. Res. Natl. Bur. Stand. (1934)* **1955**, *55*, 197.

https://dx.doi.org/10.1021/acs.nanolett.0c05059
Nano Lett. 2021, 21, 2232−2239